



ACADÉMIE  
DES SCIENCES  
INSTITUT DE FRANCE

# *Comptes Rendus*

---

## *Chimie*

Naveen Sharma, Ashutosh Patel, Raman Deep and Shivam Gautam


**Performance augmentation of triangular solar still using sensible energy storage materials: thermo-exergo-economic and sustainability analyses**

Published online: 9 December 2024

**Part of Special Issue:** Materials and Energy Valorization of Biomass and Waste : The Path for Sustainability and Circular Economy Promotion

**Guest editors:** Mejdi Jeguirim (Université de Haute-Alsace, Institut de Sciences des Matériaux de Mulhouse, France) and Salah Jellali (Sultan Qaboos University, Oman)

<https://doi.org/10.5802/crchim.346>

 This article is licensed under the  
CREATIVE COMMONS ATTRIBUTION 4.0 INTERNATIONAL LICENSE.  
<http://creativecommons.org/licenses/by/4.0/>



*The Comptes Rendus. Chimie* are a member of the  
Mersenne Center for open scientific publishing  
[www.centre-mersenne.org](http://www.centre-mersenne.org) — e-ISSN : 1878-1543



Research article

## Materials and Energy Valorization of Biomass and Waste : The Path for Sustainability and Circular Economy Promotion

# Performance augmentation of triangular solar still using sensible energy storage materials: thermo-exergo-economic and sustainability analyses

Naveen Sharma<sup>✉,\*</sup>, Ashutosh Patel<sup>a</sup>, Raman Deep<sup>✉</sup>,<sup>a</sup> and Shivam Gautam<sup>a</sup>

<sup>a</sup> Department of Mechanical Engineering, Netaji Subhas University of Technology, New Delhi-110078, India

E-mails: naveen.sharma@nsut.ac.in, sharma.naveen28@yahoo.com (N. Sharma)

**Abstract.** People in remote areas often struggle with limited access to potable water. This experimental research aims to augment the performance of a triangular solar still (TSS) by incorporating sensible heat storage materials (SHSMs) for sustainable freshwater production. Four different configurations—standard TSS, TSS with bricks (TSS-B), TSS with paper napkins wrapped around the brick (TSS-NB), and TSS with sand bed (TSS-S)—were tested under the climatic conditions of New Delhi (28° 35' N, 76° 54' E), India, during October 2023. The performance of TSS was assessed based on energy, exergy, economic, and environmental parameters. From experimental results, it was observed that the daily yield of the TSS-S was 3.12 L/m<sup>2</sup>, which is about 81.40% higher than that of TSS. Additionally, the daily yield increased by around 34.86% for TSS-B and about 28.23% for TSS-NB than TSS. Incorporating SHSMs into the TSS led to significant enhancements in energy efficiency (19.15% to 75.12%) and exergy efficiency (7.41% to 36.44%) compared to TSS, solidifying it as a viable choice for freshwater production. The economic assessment revealed that employing SHSMs resulted in a reduction in the cost per liter of freshwater generation by up to 42.86% (for TSS-S) and a corresponding decrease in the payback period by up to 44.33% (for TSS-S) compared to TSS. Furthermore, the exergetic sustainability of the TSS was explored using improvement potential and sustainability index parameters. Moreover, the TDS and pH values of the yield produced from TSS, with and without SHSMs, adhere to water quality standards.

**Keywords.** Heat storage material, Desalination, Sustainability analysis, Thermo-exergo-economic analysis, Triangular solar still.

*Manuscript received 15 March 2024, revised 7 July 2024 and 12 September 2024, accepted 24 September 2024.*

## 1. Introduction

Every living organism, including humans, plants, and animals, relies on water for its existence. Mother

Earth's most abundant resource is water, which can be found in oceans, glaciers, and groundwater. However, the water available in these sources is not in pure form; it contains some impurities, such as salt and pollutants. The amount of fresh water suitable for human consumption is less than 1%. Apart from

\*Corresponding author

drinking, there are many other uses for water in fields including agriculture and industry [1].

The current rise in population, rapid industrialization, and changing human lifestyles contribute to an intensified demand for fresh water, upsetting the natural balance of water supply. A report by UNICEF and the World Health Organization (WHO) states that in the twentieth century, more than 2.2 billion people lack access to safe drinking water worldwide [1].

Several methods are used for desalination, for instance, membrane distillation [2], reverse osmosis process, multi-stage flash, electrolysis, adsorbents for the treatment of water [3,4], and dehumidification and humidification [5]. Desalination processes currently rely on fossil fuels or electric energy, contributing to global warming in the long run. Since India enjoys a tropical climate, with approximately 250 to 330 sunny days each year, solar energy finds versatile applications such as electricity generation [6], water purification [7], air and water heating [8], and cooking and drying [9].

Solar desalination stands out as the optimal approach for freshwater production due to its simple design, utilization of eco-friendly energy, and suitability for remote locations [10]. However, solar stills (SSs) continue to demonstrate a limited level of productivity. Numerous studies have been published to augment the productivity of SSs by modifying their basic designs, including single slope, double slope, multi-effect, drum SS, and hemispherical SS [11,12]. In a recent systematic review, Bait [13] compared triangular pyramids, weir-like structures, spherical designs, and hemispherical SSs. The study focused on design modifications, heat transport fluids, sensible heat storage materials (SHSMs), collector integration, and cooling processes. It was concluded that hemispherical, weir-like, and pyramidal SSs outperformed other types.

Younis *et al.* [14] explored recent developments in SSs, including single-slope, double-slope, condenser-based, and hybrid designs. Key findings revealed that incorporating materials such as charcoal, matting, sponges, dyes, wicks, porous or energy-storing materials, black rubber, and floating absorber sheets improved basin absorption. Additionally, using inclined external flat-plate reflectors, combined stills, condensers, and solar collectors significantly enhanced productivity while minimizing heat loss.

In an experimental study by Ramzt *et al.* [15], natural and artificial materials, like black loofah, regular loofah, fine steel wool, and steel wool pads (SWPs), were used to enhance SS performance and productivity. Steel wool pads achieved the highest yield of 4.384 L/m<sup>2</sup> and the highest thermal efficiency at 32.74%. The cost per liter (CPL) was lowest with SWPs at 0.0034 \$/L/m<sup>2</sup>. Exergo-economic analysis indicated that SWPs were the most promising modification for improving SS performance.

In a research endeavor, Deshmukh and Thombre [16] conducted experiments involving a single-slope SS employing sand and Servotherm medium oil working as SHSMs. Their findings indicated that a reduced depth of the SHSM resulted in the highest distilled water production when compared to traditional stills. Interestingly, the productivity continued to rise due to SHSM even during nighttime.

Abdelgaleel *et al.* [17] explored the productivity of SSs using iron hemispherical pieces (IHPs) and SWPs. The findings indicated that productivity increases by 35% when there are 120 IHPs. Moreover, a substantial 28% increase in productivity was achieved with the addition of SWPs.

Kumar *et al.* [18] examined the performance of an integrated triangular solar still (TSS) at various water depths. The study's observations indicated that the TSS achieved maximum yield at 0.02 m water depth. The integration of the inclined SS resulted in an increased inlet water temperature, leading to the production of maximum distilled water (7.52 kg/m<sup>2</sup>). In their research on a double-basin SS, Modi *et al.* [19] explored the correlation among water depth, evaporation rate, and freshwater yield. The authors noted that the daily distilled production was higher for lower water depths, specifically 2.02 and 1.79 L/m<sup>2</sup> with water depths of 0.01 m and 0.04 m, respectively, in the lower basin.

Furthermore, Kabeel *et al.* [20] studied the impact of water depth (0.02–0.06 m) on the freshwater yield of standalone conventional, inclined, and integrated conventional and inclined SSs. The findings revealed a significant 46.23% increase in yield with the integrated SS. Moreover, it was noted that the maximum accumulated distilled water was observed when the water depth was maintained at 0.02 m. In a related study, Manokar *et al.* [21] explored the impact of water depth and insulation on pyramidal acrylic SSs. The daily yield of

the SS experienced a 28% enhancement at a water depth of 0.01 m.

Physical parameters play a pivotal role in augmenting the productivity of SSs. Studies by Azooz and Younis [22] and Kabeel *et al.* [23] investigated the effect of glass cover inclination on the distillate output of single-slope and pyramidal SSs, respectively. Both studies demonstrated that higher inclinations resulted in lower productivity.

Feilizadeh *et al.* [24] inspected the impact of dimensional parameters on the effectiveness of a single-slope, single-basin SS. The authors revealed that higher specific height resulted in lower productivity, with the optimal height for the still being around 0.10 m. Additionally, maintaining a width-to-length ratio of about 0.4 led to maximum productivity. In another study conducted by Jamil and Akhtar [25] in an indoor setting, the impact of specific height (varying from 0.266 to 0.341 m in increment of 0.025 m) on a conventional SS was investigated. Their results revealed a noteworthy 50% increase in productivity when the specific height was reduced from 0.341 m to 0.266 m.

Recently, Bait *et al.* [26] developed a new design of SS that embeds a simple distiller into a cylindrical solar collector shape. This collector raises the basin water temperature by 31% and 40% for passive and active solar stills, respectively, resulting in increased yield and energy efficiency.

Furthermore, modifying the absorbing area represents another approach to increase the effectiveness of SSs. Appadurai and Velmurugan [27] scrutinized the impact of using fin-type solar ponds on the performance of SS. Their observations revealed that the use of fins increased the area available for heat transfer, causing a substantial 45.5% increase in daily distilled water production. Additionally, their study on fins in a solar pond showed a productivity increase of approximately 27.6%. In an analogous manner, El-Naggar *et al.* [28] observed the effect of fins on SSs and noted a significant 55.37% increase in daily distilled water output. Moreover, Sharma *et al.* [29] inspected the enhancement of freshwater production in pyramid-shaped SSs by incorporating copper tube fins spaced at 9 cm and 14 cm. The study indicated a 60% improvement in yield with fins at a spacing of 9 cm and a 33% improvement at 14 cm compared to an SS without fins. Tuly *et al.* [30] considered the combined influence of phase change

material (PCM), nanoparticles, and fins in a double-slope SS. Their findings indicated a substantial increase in productivity as well as energy and exergy efficiencies. Specifically, the modified experimental setup demonstrated a noteworthy 20.1% and 25% increase in energy and exergy efficiencies, respectively. In a recent study, Panchal *et al.* [31] made improvements to the single-slope SS by incorporating perforated fins, pebbles, and an evacuated tube solar collector. Experimental results demonstrated remarkable improvements: productivity increased by 244.1%, thermal efficiency rose by 2.32%, and the CPL decreased by 10%. Furthermore, the modified SS achieved nearly 2.44 times the CO<sub>2</sub> mitigation value than the standard configuration.

Employing porous and heat storage materials represents an alternative approach to augment SS performance. Kabeel and Abdelgaied [32] incorporated PCM to augment the distillate output of a single-basin SS, reporting a substantial improvement. The daily yield increased by 67.18%. Shalaby *et al.* [33] introduced a v-corrugated absorber SS incorporating PCM and explored the impact of providing a wick material over the absorber plate. By employing PCM, the daily performance showed a notable 12% improvement compared to the v-corrugated basin alone. The authors noted a slight decrease in daytime productivity when using PCM, coupled with a significant escalation in overnight yield. Specifically, the diurnal yield of the SS with PCM was reported to be 11.7% higher than that of the v-corrugated still with PCM and wick material.

Abdel-Aziz *et al.* [34] aimed to enhance the effectiveness of an SS by using paraffin wax as a PCM and a solar-powered electric heater. The experimental findings indicated that activating the heater within the PCM resulted in a daily yield increase of 2.38, 2.66, and 3.1 times during spring and 2.2, 2.39, and 2.67 times during summer, compared to the conventional SS. The highest daily production occurred in both seasons (spring and summer) when the temperature of the paraffin wax was maintained at 65 °C.

Additionally, Shoeibi *et al.* [35] aimed to improve the operational effectiveness of solar desalination systems by using mirrors, waste thermoelectric generators, and black iron fragments as SHSMs. During the study, two thermoelectric generators were attached to the basin to harness electrical energy within the absorber plate. The results indicated that

conventional SS, SS-TEG, SS-TEG-WI, and SS-TEG-WI-M produced fresh water at rates of 0.64 L/m<sup>2</sup>, 0.63 L/m<sup>2</sup>, 0.652 L/m<sup>2</sup>, and 0.796 L/m<sup>2</sup>, respectively.

In an experimental investigation, Hemmatian *et al.* [36] used pulsating heat pipes, evacuated solar collectors, and PCM to enhance yield during low solar irradiation. The system, which employs paraffin wax as the PCM, produces 2248 mL/m<sup>2</sup>, resulting in a 40% increase in daily freshwater production compared to conventional SS. Additionally, the system reduces CO<sub>2</sub>, SO<sub>2</sub>, and NO emissions and exhibits energy efficiencies of 19.4% for solar stills using heat pipes (SSHP) and 20.3% for solar stills employing pulsating heat pipes (SSPHP). The exergy-economic factors for conventional SS, SSHP, and SSPHP are 1.27 kWh/\$, 1.56 kWh/\$, and 1.62 kWh/\$, respectively.

Shoeibi *et al.* [37] tested a modified single-slope SS integrated with a photovoltaic panel, heat pipes, and a thermoelectric generator to improve performance and efficiency. The daily water productivity values for conventional SS, solar still with a wick structure (SS-WT), solar still with heat pipes (SSHP), and solar still with heat pipes and a wick structure were approximately 0.748 L/m<sup>2</sup>, 0.832 L/m<sup>2</sup>, 1.058 L/m<sup>2</sup>, and 1.162 L/m<sup>2</sup>, respectively. Omid *et al.* [38] investigated a hybrid system that mitigates pollution by utilizing a parabolic-trough heat pipe solar collector. The study found that water flow rate, length of the porous medium, and the number of heat pipes significantly affect energy efficiency. The system achieved its highest recorded daily output of 4.940 L/day.

Furthermore, Shanmugan *et al.* [39] examined the theoretical and practical performance of SS by employing wick materials in conjunction with a PCM and nanoparticles. The findings indicated that the yields of wick materials in an SS with PCM and nanoparticles were 7.460 L/m<sup>2</sup> and 4.120 L/m<sup>2</sup>, respectively. In a study by El *et al.* [40], the traditional hemispherical solar still was investigated with a TiO<sub>2</sub> nanocoated tank and glass cooling. The daily energy efficiency values for a coated basin at concentrations of 0.1%, 0.2%, and 0.3% with glass cooling are 40.34%, 46%, and 51%, respectively. Shoeibi *et al.* [41] investigated the effectiveness of SSs that utilize Al<sub>2</sub>O<sub>3</sub> nanofluid film cooling to enhance yield. The results indicated that double-slope SSs with nanofluid film cooling increased yield by 4.8% compared to tubular desalination. Dual-slope solar desalination with nanofluid film cooling provides CPL at 0.0362 \$/L.

Kabeel *et al.* [42] used jute cloth wrapped around sand for heat storage. Their findings showed a 25% improvement in efficiency, accompanied by a freshwater yield of 5.9 L/m<sup>2</sup> when utilizing jute cloth. Pal *et al.* [43] created a thermal model for a modified multi-wick double-slope SS. The researchers observed peak values for instantaneous energy and exergy efficiencies, reaching 35% and 3.83% at 5:00 p.m., respectively. Additionally, the annual reduction in CO<sub>2</sub> emissions was determined to be 7.82 tons with jute wicks and 8.69 tons with black cotton wicks, at 0.01 m water depth. Yousef *et al.* [44] explored the energy, exergy, economic and enviroeconomic aspects of single-slope SS using various absorbing materials. Their findings revealed that the SS with steel wool fibers exhibited a 25% increase in daily water yield, while the SS with hollow cylindrical pin fins showed a 16% enhancement.

Manokar *et al.* [45] conducted an experimental investigation on a modified single-slope SS incorporating base heating and glass cooling. Experimental findings revealed notable improvements, with a 24.03% increase in yield, a 25% enhancement in energy efficiency, and an 18.9% boost in exergy efficiencies when employing glass cooling. Additionally, the application of the base heating method resulted in even more substantial improvements, with a 50.11% increase in yield, along with 50.66% and 59.61% enhancements in energy and exergy efficiencies, respectively.

Elashmawy [46] examined the influence of small-sized gravel (3 kg) as SHSMs on tubular SSs. The study demonstrated a significant improvement in efficiency and daily productivity, with increases of 36.34% and 4.51 L/m<sup>2</sup>, respectively, against the scenario without gravel. Furthermore, Kabeel *et al.* [47] delved into the performance of tubular SSs featuring v-corrugated basin plates with wick material. The findings showcased a substantial daily average efficiency boost of 46.86% with the incorporation of wick material. Shoeibi *et al.* [48] examined the use of porous materials in solar water desalination systems and reported that activated carbon increases energy efficiency by 94.14%, whereas black steel wool fibers and aluminum fins increase output by 42.3% and 20.9%, respectively.

In a separate investigation, El *et al.* [49] explored productivity enhancements in a traditional SS by incorporating sandbags as solar radiation absorbers,

functioning as SHSMs. The results indicated a noteworthy productivity increase of approximately 34.57%. Dhivagar [50] evaluated the influence of magnetic powder as an SHSM. Specifically, black iron oxide magnetic powder was employed to augment the productivity of SS. The outcomes revealed a remarkable 32% enhancement in the effectiveness of the magnetic-powder-equipped SS, with significant enhancements observed in both exergy and energy.

Mevada *et al.* [51] conducted experimental research on the impact of SHSM on performance, along with an analysis of energy and exergy efficiency. The incorporation of SHSM increased the rate of distillate water output. The energy and exergy efficiency were measured as 43.29% and 12.55%, respectively, surpassing the values achieved by conventional SSs. In an experimental study, Bait [52] compared the performance of conventional and modified SSs and showed that the annual yield for the modified SS is approximately 405.04 kg/m<sup>2</sup>, while the conventional SS yields around 549.77 kg/m<sup>2</sup>. The payback period for the conventional SS was approximately 7.7 years, whereas the modified SS had a payback period of approximately 21 years.

Shoeibi *et al.* [53] explored a novel configuration for solar desalination that incorporated thermoelectric elements on both the cold and hot sides. During the experiment, ambient air flowed through a cooling tank and a water heater block connected to the hot side. The results revealed significant improvements in freshwater yield (79.4%), energy efficiency (11.2%), and exergy efficiency (45.7%).

For the purpose of improving freshwater yield and enhancing environmental sustainability, Dhivagar *et al.* [54] examined mussel shell biomaterial as a porous medium and SHSM in a SS. Mussel shells absorb solar radiation and store solar thermal energy, raising the water's temperature. It was found that SS with mussel shell biomaterial had superior energy efficiency (10.3%) and exergy efficiency (9%), and reduction in CO<sub>2</sub> emissions (11.1%) and CPL (10.9%) to conventional SS.

Recently, Mahala and Sharma [55] proposed an innovative design of pyramid SS with HSMs that results in significant improvement of daily yield (84%), energy efficiency (81.1%), and carbon credits earned (76%) along with substantial reduction in CPL of yield produced (29.2%) and payback period (29%) when compared with conventional SS.

The pertinent literature indicates that SSs exhibit low productivity, making their commercialization challenging in the domestic sector. Consequently, various active and passive techniques have been employed to enhance the yield produced and energy efficiency of SSs. Despite extensive literature, comparative studies on TSS using bricks and wicking materials as SHSMs are lacking. Additionally, the use of sand as a bed is not adequately covered. Taking a step forward, this study explores the use of SHSMs to increase the performance of TSS. The goal is to ensure a sustainable supply of fresh water even during periods without direct sunlight. Typically, SHSMs accumulate thermal energy during peak sunshine hours and gradually release it when solar intensity decreases. This research investigates and compares the effectiveness of TSS with different SHSM configurations, including the standard TSS, TSS with bricks (TSS-B), TSS with paper napkins wrapped around the brick (TSS-NB), and TSS with a sand bed (TSS-S). The comparison considers performance parameters, such as freshwater yield, energy efficiency, exergy efficiency, and economic factors. Additionally, the key metrics like "improvement potential" and "sustainability index" are employed to assess the exergetic sustainability of each configuration. Furthermore, the study involves measuring and comparing total dissolved solids (TDS) and pH levels in the raw water and the produced yield. These findings enhance the existing benchmark dataset for SS systems.

## 2. Experimental details

The present experimental facility, depicted in Figure 1, was developed at NSUT West Campus, New Delhi. The experiments were carried out between 8:00 a.m. and 7:00 p.m. during October 2023. The test rig comprises a triangular wooden basin with an internal absorbing area of 0.43 m<sup>2</sup>. Each side of the basin, with a height of 0.3 m, is covered with galvanized iron sheet, acting as an absorber plate, with black coating (absorptivity of 0.95) to augment the absorption of solar radiation. The TSS basin is insulated from the sides and bottom by using a 20 mm wooden box for decreasing the heat loss to the surroundings. In the basin, 7 L of saline water is filled. A water level indicator is used to ensure a constant amount of water. A drainage valve at the bottom facilitates the removal of contaminated water and

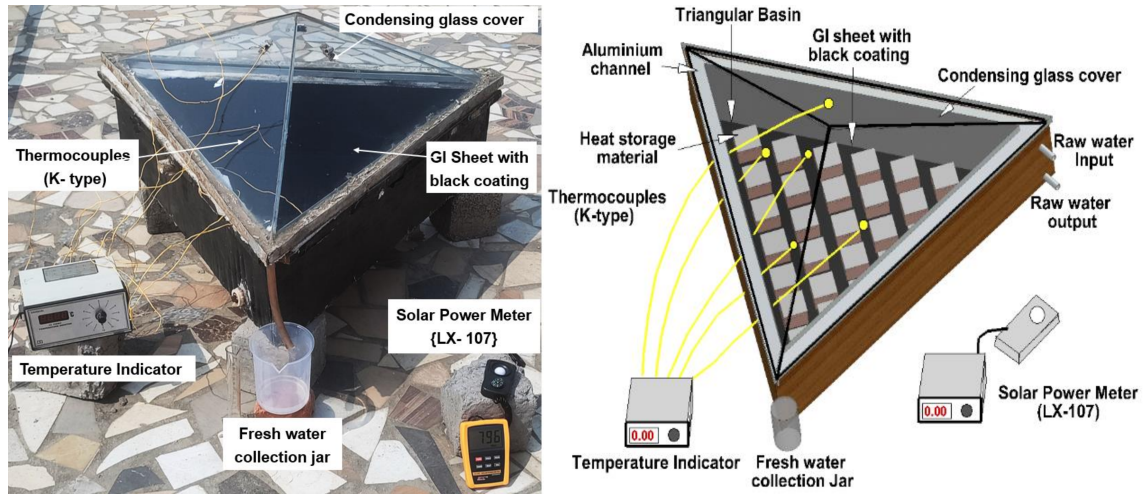


**Figure 1.** Photograph and schematic of the experimental test rig.

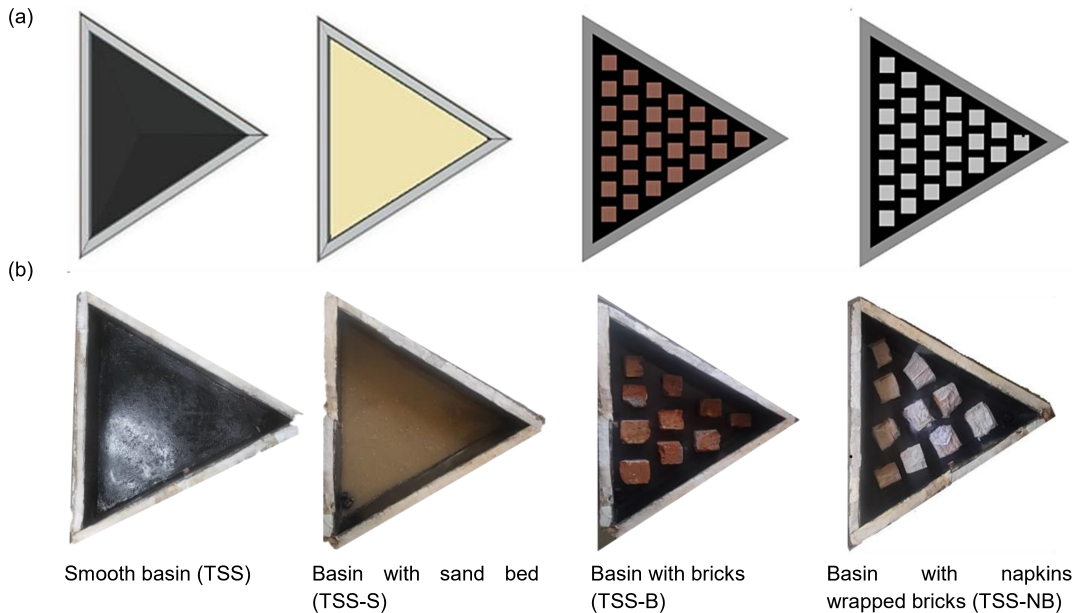


**Figure 2.** (a) Schematic and (b) images of studied configurations.

cleaning. A 3 mm thick triangular pyramidal glass cover serves as a condensing cover.

Solar radiation penetrates the glass cover, heating the basin water and generating water vapor. These vapors condense on the inner side of the glass cover due to its lower temperature. To collect the yield output, a calibrated flask is utilized.

The study investigates the performance of four distinct configurations with and without heat stor-

age, namely TSS, TSS-B, TSS-NB, and TSS-S, illustrated in Figure 2. Coarse sand and bricks are used as heat storage materials. Given the critical role of SHSMs in SS productivity, a constant mass of approximately 15 kg was maintained throughout the experiment. Due to its high thermal mass, SHSM absorbs and retains heat during the day and radiates it out at night. Productivity comparison is made only for days with almost similar solar radiation

**Table 1.** Thermophysical properties of the SHSMs

Material	Density (kg/m <sup>3</sup> )	Specific heat (J/(kg·K))	Thermal conductivity (W/(m·K))	Emissivity coefficients
Bricks [56]	1500–1800	840	0.9–1.2	0.74–0.93
Sand [57]	1600–1700	932–958	0.2–0.7	0.7–0.9
Paper napkin [58]	0.62–1.26	1.52	0.08–0.18	0.6–0.93

**Table 2.** Instruments with their uncertainty

Tools	Range ± precision	Error
Solar power meter (LX-107) <sup>a</sup>	0–2000 ± 5	±2.88
Collecting flask <sup>b</sup>	0–1000 ± 50	±28.87
Temperature display <sup>c</sup>	0–1200 ± 1	±0.58
Thermocouple <sup>d</sup>	0–1200 ± 1	±0.58
pH Meter	0–14 ± 0.01	±0.0058
TDS meter <sup>e</sup>	0 to 2000 ± 2%	±1.155

<sup>a</sup> Solar radiation measured in W/m<sup>2</sup>.

<sup>b</sup> Distillate output measured in mL.

<sup>c</sup> Temperature displayed in °C.

<sup>d</sup> Temperature measured in °C.

<sup>e</sup> TDS measured in ppm.

intensity and at the constant amount of raw water. Table 1 presents the thermophysical properties of the SHSMs.

Solar radiation is quantified using a solar power meter with an accuracy of ±5. K-type thermocouples are placed at different positions to monitor temperatures including the basin, water, vapor, condenser glass, and ambient. Hourly data recording is performed manually using a digital temperature indicator. Hourly measurements of the produced fresh water are made with a calibrated flask. Additionally, pH and TDS meters are utilized to assess the quality of both saline and purified water. Table 2 outlines the precision, range, and typical uncertainty of the measurements (uncertainty = precision/√3) [55].

Following the procedure adopted by Mahala and Sharma [59], the uncertainties in hourly yield and overall daily yield were determined to be ~1.5% and ~2.1%, respectively. Additionally, considering the uncertainties in solar radiation measurement, daily yield, and temperature measurement, there was an

associated error of approximately ±2.8% in energy efficiency and ±3.2% in exergy efficiency.

### 3. Data reduction

#### 3.1. Energy analysis

The hourly basis thermal energy efficiency of the TSS is obtained by [59]

$$\eta_{en} = \frac{\sum m_w \times h_{fg}}{A_t \int I_S(t) dt} \times 100 \quad (1)$$

$$h_{fg} = 2.4935 \times 10^6 [1 - 9.478 \times 10^{-4} T_w + 1.31 \times 10^{-7} T_w^2 - 4.79 \times 10^{-9} T_w^3] \quad (2)$$

Here,  $m_w$  represents the distillate output (L/m<sup>2</sup>),  $I_S$  denotes solar irradiation (W/m<sup>2</sup>),  $A_t$  refers to the TSS area (m<sup>2</sup>), and  $h_{fg}$  indicates latent heat of evaporation in the case of water (J/kg).

#### 3.2. Exergy analysis

The exergy efficiency for TSS is determined by [60]

$$\eta_{ex} = \frac{E_{x,out}}{E_{x,in}} \quad (3)$$

The output exergy and the exergy input of the TSS can be found from Equations (4) and (5), respectively:

$$\sum E_{x,in} = I_S \times A_t \left[ 1 - \frac{4}{3} \left( \frac{T_{amb}}{T_{sun}} \right) + \frac{1}{3} \left( \frac{T_{amb}}{T_{sun}} \right)^4 \right] \quad (4)$$

$$\sum E_{x,out} = m_w \times h_{fg} \times \left[ 1 - \left( \frac{T_{amb}}{T_w} \right) \right] \quad (5)$$

where  $T_{sun}$  is the sun temperature (6000 K) and  $T_{amb}$  is the ambient temperature [37].

#### 3.3. Economic analysis

The cost breakdown for each component of TSS across all studied configurations, as depicted in Figure 2, is detailed in Table 3. The economic analysis parameters and equations are outlined below [59].



Let  $C_{in}$  represent the initial cost spent in the construction of TSS, with an annual interest rate ( $i$ ) of 8%, and  $n$  denote the lifespan of TSS ( $n = 15$  years). The capital recovery factor and annual fixed cost ( $C_{AFC}$ ) are computed as follows:

$$\text{Capital recovery factor} = \frac{i(1+i)^n}{(1+i)^n - 1} \quad (6)$$

$$C_{AFC} = C_{in} \times \text{Capital recovery factor} \quad (7)$$

Annual operational and maintenance cost ( $C_{AOMC}$ ), encompassing expenses for regular cleaning, feed water filling, freshwater collection, and scaling removal due to salt deposition inside the TSS, is set at 15% of  $C_{AFC}$ :

$$C_{AOMC} = 0.15(C_{AFC}) \quad (8)$$

Consequently, the annual salvage cost ( $C_{ASV}$ ) is determined as

$$C_{ASV} = 0.20 C_{in} \times \frac{i}{(1+i)^n - 1} \quad (9)$$

The total annual cost ( $C_{TAC}$ ) is computed by

$$C_{TAC} = C_{AFC} + C_{AOMC} - C_{ASV} \quad (10)$$

Annual freshwater yield ( $M_a$ ) in  $L/m^2$  is evaluated using

$$M_a = m_w \times N_d \quad (11)$$

where  $m_w$  denotes the mean daily freshwater yield per unit area and  $N_d$  indicates the number of sunny days (330 days for New Delhi).

“Cost per liter” of yield generated ( $C_{CPL}$ ) is estimated as

$$C_{CPL} = \frac{C_{TAC}}{M_a} \quad (12)$$

Annual market cost of yield ( $C_{AMA}$ ) is calculated as

$$C_{AMA} = M_a \times \text{Market cost of water per liter} \quad (13)$$

Net annual earnings ( $C_{AE}$ ) is determined by

$$C_{AE} = C_{AMA} - C_{AOMC} \quad (14)$$

The payback period ( $P_p$ ), in days, for the TSS is calculated by

$$P_p = \frac{C_{in}}{C_{AE}} \times 365 \quad (15)$$

### 3.4. Sustainability index

The efficiency with which a system utilizes its resources is called sustainability index (SI). The following formula is used to determine the sustainability index [61].

$$SI = \frac{1}{1 - \eta_{ex}} \quad (16)$$

**Table 3.** Fabrication cost of each TSS (\$)

Component of TSS	TSS	TSS-B	TSS-NB	TSS-S
Glass cover	17.96	17.96	17.96	17.96
Absorber plate (GI)	20.96	20.96	20.96	20.96
Wooden frame	26.35	26.35	26.35	26.35
Collecting jar	2.99	2.99	2.99	2.99
Aluminum frame	2.99	2.99	2.99	2.99
Black paint	2.99	2.99	2.99	2.99
PVC pipe	1.80	1.80	1.80	1.80
Insulation	1.80	1.80	1.80	1.80
Heat storage material				
Sand	–	–	–	1.79
Napkins	–	–	0.23	–
Bricks	–	2.99	2.99	–
Total cost (\$)	77.84	80.84	81.08	79.64

### 3.5. Improvement potential

Reducing irreversibility within a system contributes to an enhancement in exergy efficiency. The subsequent equation is employed to calculate the improvement potential (IP) [62].

$$IP = (1 - \eta_{ex})^2 \times E_{x,in} \quad (17)$$

## 4. Results and discussion

Experiments for different configurations—TSS, TSS-B, TSS-NB, and TSS-S—are carried out between 8:00 a.m. and 7:00 p.m. Experimental data related with temperatures at strategic locations, along with measurements of solar radiation intensity and distillate yields on an hourly basis, are recorded manually. Figure 3 illustrates hourly variation in solar intensity and ambient temperature for the studied configurations in October 2023. As expected, solar radiation gradually increases during the forenoon hours, reaching its peak value at 12:00 p.m., and gradually decreases in the afternoon, reaching its lowest point at sunset around 6:00 p.m. Figure 3 also shows that the ambient temperature follows a similar trend, rising concurrently with solar radiation in the forenoon and declining in the afternoon. The average solar intensity and ambient temperature measured are approximately  $285 \text{ W/m}^2$  and  $36 \text{ }^\circ\text{C}$ , respectively.

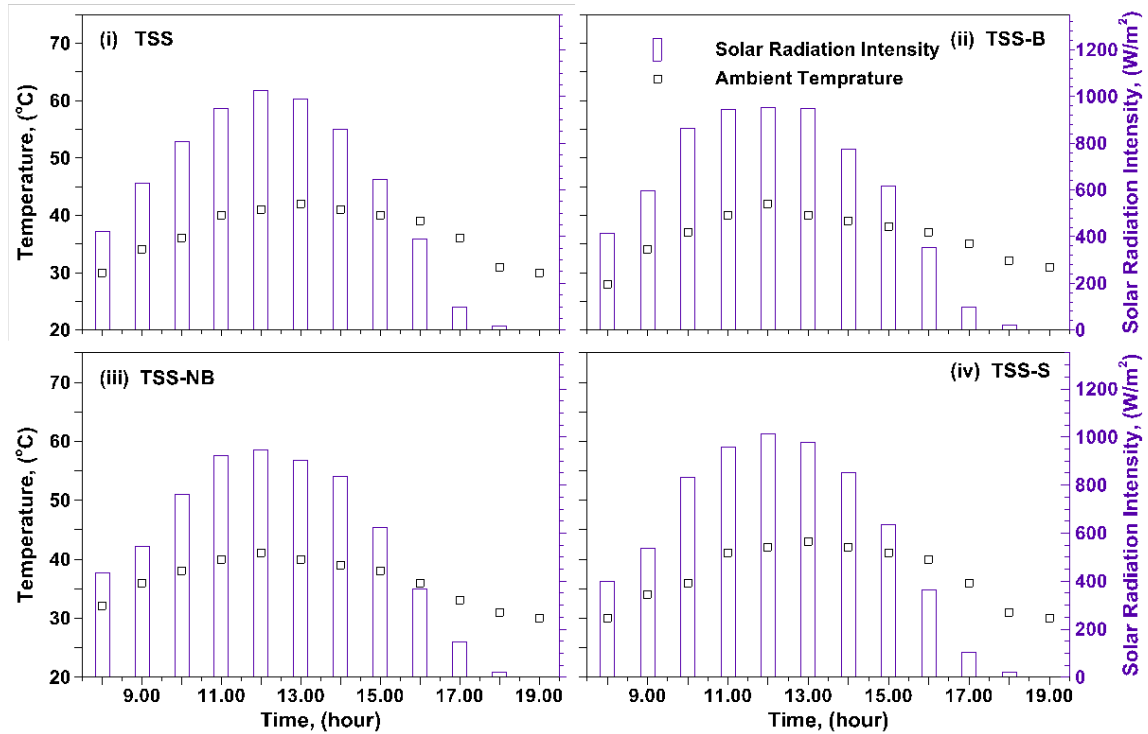


**Figure 3.** Ambient temperature and solar intensity variation for different configurations.

Notably, the variabilities in solar irradiance and ambient temperature during the experimental days fall within  $\pm 2.5\%$ . The average wind speeds for the four days were 9.85 km/h, 8.45 km/h, 9.27 km/h, and 8.96 km/h, indicating that the fluctuations during the experimental days remained within  $\pm 5\%$ . Consequently, the obtained recorded data for the four configurations can be equated to assess the effectiveness of SHSMs in enhancing the performance of the TSS.

Figure 4 illustrates the hourly variation in temperature associated with the studied configurations. For TSS, the peak temperatures observed are 65 °C for water, 66 °C for the basin, and 58 °C for the glass. The average temperature dissimilarity between water and glass is 3 °C, creating the necessary conditions for vapor condensation over the inner glass surface. Due to the absence of SHSMs, water and basin temperatures rise rapidly in the forenoon and decline rapidly in the afternoon for TSS. In the case of TSS-B, the maximum temperatures recorded are 58 °C for water, 62 °C for the basin, and 57 °C for the glass. The use of bricks as SHSM leads to lower temperatures compared to

TSS during daytime, as the bricks absorb a portion of solar radiation. In addition, the release of the absorbed heat by the bricks in the evening hours results in a lower temperature drop for TSS-B compared to TSS, leading to higher productivity during the evening.

For TSS-NB, the highest temperatures are 58 °C for water, 59 °C for the basin, and 60 °C for the glass. The presence of napkins wrapped over bricks reflects a considerable part of solar intensity to the glass cover, increasing the glass temperature in the forenoon. Although TSS-NB has a slightly higher glass temperature compared to the other cases, it decreases as solar intensity declines in the afternoon.

In the case of TSS-S, peak temperatures are 55 °C for water, 60 °C for the basin, and 54 °C for the glass. TSS-S, with the highest mass of SHSM, absorbs a significant portion of solar intensity initially and radiates it during the night. Consequently, all temperatures in TSS-S remain lower compared to TSS.

Figure 5 illustrates the hourly variation in distillate productivity for the investigated configurations. Typically, the hourly yield from the SS is primarily

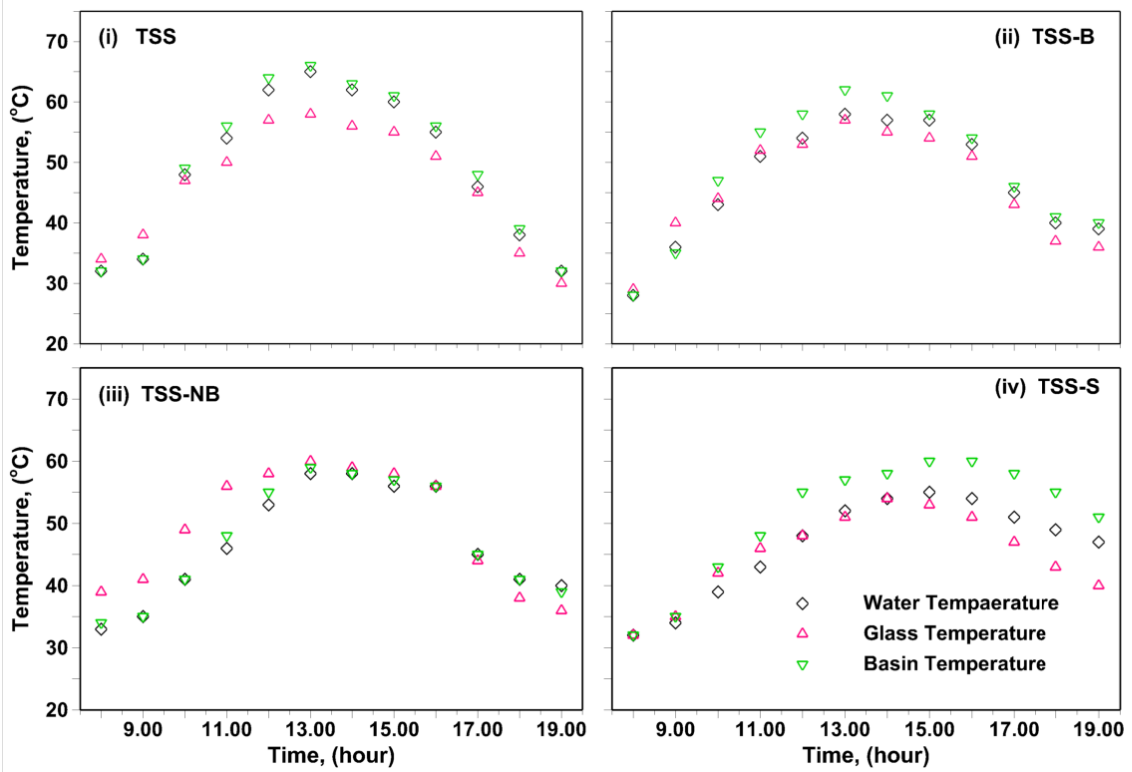


**Figure 4.** Hourly temperature variations within a solar still for different configurations.

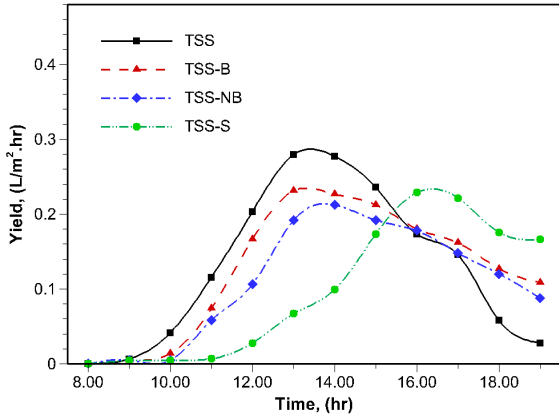


**Figure 5.** Variation in yield for different configurations.

influenced by solar intensity and the temperature difference between water and glass. Figure 5 shows that the yields of all examined cases closely align in the beginning. As time advances, the yield pro-

duction rate diminishes during the forenoon hours due to the introduction of thermal mass, specifically SHSMs. However, post 3:00 p.m., there is a shift in productivity trends, with TSS-S exhibiting a higher yield. The solar energy absorbed by bricks and sand in the early part of the day elevates water temperature after 3:00 p.m., as depicted in Figure 4, consequently enhancing rates of evaporation and condensation.

Figure 6 depicts the variation in daily productivity across all four configurations. During the daytime, TSS generates the highest quantity of yield, specifically 1.56 L/m<sup>2</sup>, followed by TSS-B with 1.51 L/m<sup>2</sup>, TSS-NB with 1.32 L/m<sup>2</sup>, and TSS-S with 1.18 L/m<sup>2</sup>. The rise in thermal mass due to SHSMs is linked to the reduction in yield production rates in the daytime. This is attributed to the increased absorption of solar energy by SHSMs. Evidently, the yield output for TSS-NB is about 14% lower than that of TSS-B owing to higher glass cover temperature as can be seen in Figure 4.

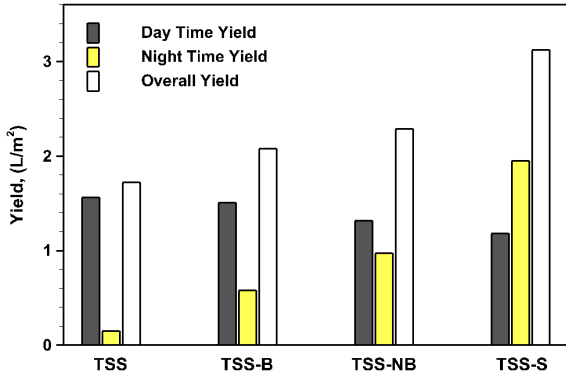


**Figure 6.** Cumulative yield comparison.

During the night, TSS-S exhibits the highest productivity of  $1.95 \text{ L/m}^2$ , while TSS-NB, TSS-B, and TSS demonstrate productivities of  $0.97 \text{ L/m}^2$ ,  $0.58 \text{ L/m}^2$ , and  $0.15 \text{ L/m}^2$ , respectively. The utilization of SHSMs results in a notable improvement in nighttime productivity, ranging from 287% to 1200%.

A more in-depth examination of Figure 6 indicates that TSS-S takes the lead by providing the highest overall yield, reaching  $3.12 \text{ L/m}^2$ , followed by TSS-NB at  $2.29 \text{ L/m}^2$ , TSS-B at  $2.08 \text{ L/m}^2$ , and TSS at  $1.72 \text{ L/m}^2$ . Notably, TSS-S exhibits yield levels approximately 81.40%, 50%, and 36.24% higher than those of TSS, TSS-B, and TSS-NB, respectively. The higher thermal mass of TSS-S allows it to store more radiation and elevate the evaporation rate throughout the night, resulting in maximum yield during nighttime hours. Evidently, napkins serve as evaporating agents for TSS-NB, thereby increasing the evaporation rate during the night, and as the glass temperature decreases in the evening, the yield rises. Overall, TSS-NB demonstrates a yield that is 33% and 10% higher than that of TSS and TSS-B, respectively.

Conclusively, SHSMs boost heat transfer rates during the evening, elevating water temperatures and consequently maximizing freshwater yield through increased evaporation rates. Incorporating SHSMs into TSS (TSS-S) results in a notable 81.40% enhancement in freshwater yield compared to TSS, establishing it as a promising choice for sustainable freshwater production.

The comparison of the overall efficiency for all four configurations—TSS, TSS-B, TSS-NB, and TSS-S—is depicted in Figure 7. The efficiency of TSS is determined by the distilled water output and the

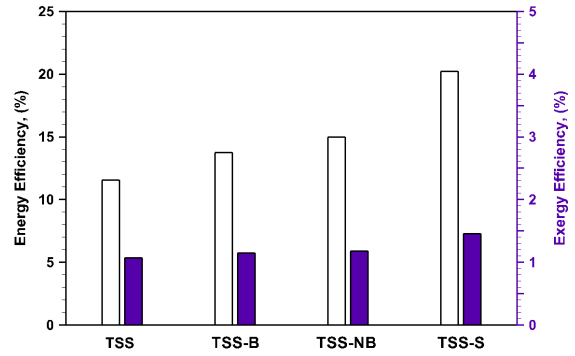


**Figure 7.** Comparison of energy and exergy efficiency.

absorbed solar irradiation. Figure 7 illustrates that the efficiency of TSS-S surpasses that of TSS, TSS-B, and TSS-NB. This is likely attributed to the higher water temperature and lower glass temperature, resulting in an elevated evaporation rate during the night and consequently yielding maximum output. The efficiencies for TSS, TSS-B, TSS-NB, and TSS-S are 11.54%, 13.75%, 14.97%, and 20.21%, respectively. Remarkably, the efficiency of TSS-S is approximately 75.12% higher than that of TSS.

The exergy, as calculated from Equation (3), is influenced by both ambient and basin water temperatures. Figure 7 reveals that TSS-S exhibits the highest exergy efficiency at 1.46%, marking 36.44%, 26.95%, and 25.86% increases compared to TSS, TSS-B, and TSS-NB, respectively. The higher basin water temperature during the night in TSS-S generates more exergy. TSS-B and TSS-NB have relatively higher basin temperatures than TSS, thereby resulting in higher exergy efficacy of approximately 7.41% and 8.67%, respectively.

Furthermore, the economic analysis assesses the viability of the TSS. The pricing of each TSS component, influenced by its local market value, plays a significant role in the overall investment. Table 4 presents the cost analyses for all considered TSS configurations.

The effectiveness of studied SSs is evaluated by comparing the CPL of freshwater generation and the payback period, as illustrated in Figure 8. The CPL of distillate yield varies for different configurations: TSS (Rs. 1.4), TSS-B (Rs. 1.2), TSS-NB (Rs. 1.1), and TSS-S (Rs. 0.8). Additionally, the corresponding payback periods for TSS, TSS-B, TSS-NB, and TSS-S

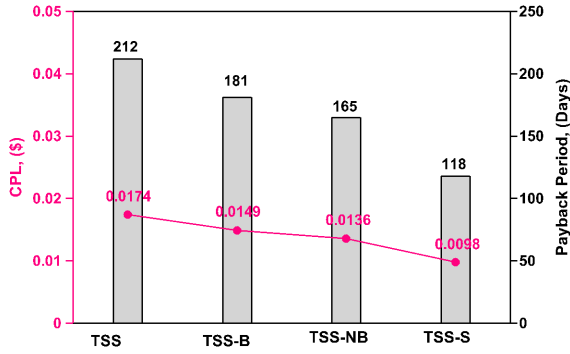


**Figure 8.** Variation in cost per liter of water and payback period for different configurations.

**Table 4.** Cost estimation corresponding to individual configurations

Economics comparison	TSS	TSS-B	TSS-NB	TSS-S
$C_{in}$ , in \$	77.84	80.84	81.08	79.64
$C_{AFC}$ , in \$	9.03	9.38	9.40	9.23
$C_{AOMC}$ , in \$	1.35	1.40	1.41	1.38
$C_{ASV}$ , in \$	15.57	16.17	16.22	15.93
$C_{TAC}$ , in \$	9.82	10.19	10.23	10.05
$M_a$ , in L/m <sup>2</sup>	~564	~686	~752	~1029
$P_p$ , in days	212	181	165	118

are 212 days, 181 days, 165 days, and 118 days, respectively.

In comparison to all investigated configurations, TSS-S emerged as the most cost-effective desalination method, as it has the lowest CPL, about 42.86% lower than TSS. In addition, the TSS-S also exhibited the least payback period, approximately 94 days lesser than TSS followed by TSS-NB and TSS-B. In summary, the desalination system incorporating SHSMs exhibited enhanced economic performance, whether augmented with sand or bricks (with and without napkins) within the system.

Figure 9 illustrates the IP and SI for all four configurations under study. The IP for investigated configurations ranges from 98.63 to 98.85. By emphasizing IP, researchers can enhance process efficiency, reduce waste, and maximize resource utilization. Increased productivity and cost savings are the ultimate outcomes of such improvements. Notably, the

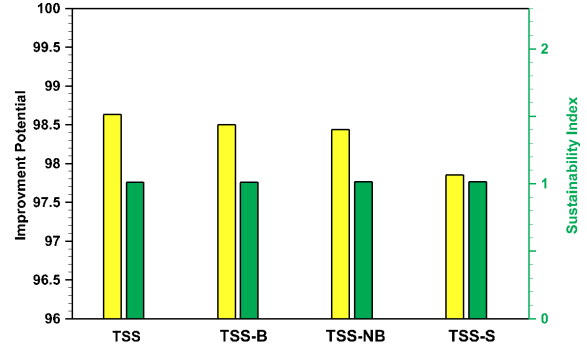


**Figure 9.** Improvement potential and sustainability indices for different configurations.

IP varies between 98.63 (lowest for TSS-S) and 98.85 (highest for TSS), indicating that TSS offers greater room for improvement while TSS-S offers the least.

The SI for investigated configurations is within the range of 1.01 to 1.014. The SI can take any positive value ranging between 1 and  $\infty$ . A higher SI signifies a reduced environmental impact per unit of production. It represents approaches that optimize renewable energy utilization, minimize waste, and decrease energy consumption. Clearly, the SI value for TSS-S is the highest (1.014). This indicates that the TSS-S utilizes solar energy more effectively than other configurations.

As indicated in Table 5, the distilled water yielded by TSS exhibits a TDS concentration ranging from 42 to 156 mg/L and a pH level between 7.2 and 7.4. These values fall within the recommended range established by the WHO, and therefore, the water is suitable for various household applications.

## 5. Performance comparison with pertinent literature

The performance parameters, namely, the productivity improvement and CPL of fresh water produced, are compared. The performance comparison is presented in Table 6, with the available literature of SSS having different types of heat storage materials for evaluating the performance of the investigated configurations. The findings indicate that the yields in this study are relatively better or comparable than those reported in previous benchmarks in the field. Furthermore, the configurations investigated in the

**Table 5.** Comparison of water quality parameters

Parameters	Before desalination	After desalination				WHO recommendation
		TSS	TSS-B	TSS-NB	TSS-S	
pH	6.1	7.3	7.3	7.4	7.2	6.5–8.5
TDS (mg/L)	1236	42	56	58	156	50–300

**Table 6.** Performance comparison of this study with relevant existing literature

S. No.	Authors	Type of solar still	HSMs	Productivity improvement (%)	CPL (\$)
1	Deshmukh and Thombre [16]	Single slope	Sand and Servotherm medium oil	6.25	–
2	Kumar et al. [18]	Triangular pyramid + single slope	Water	79.05	–
3	Kabeel et al. [42]	Single slope	Sandbag and jute cloth	25.24	–
4	Yousef et al. [44]	Single slope	Sandbag	35.24	0.04
5	El et al. [49]	Single slope	Sandbags	34.57	2.31
6	Dhivagar [50]	Single slope	Magnetic powder	31.22	0.02
7	Mahala and Sharma [55]	Square pyramid	Gravels & PCM	84.00	0.22
8	Current study	Triangular pyramid	TSS-B	36.24	0.0149
			TSS-NB	50.00	0.0136
			TSS-S	81.41	0.0096

present study are superior and commendable compared to others due to their lower CPL.

## 6. Conclusions

The current investigation assesses the performance of TSSs based on thermo-exergo-economic and sustainability analyses. Based on the experimental outcomes, the following insights can be drawn:

- The distilled water output in TSS is significantly influenced by the mass of SHSMs and the area of solar radiation absorption. Additionally, ambient temperature and glass temperature play crucial roles in distilled water production.
- The integration of SHSMs with TSS resulted in increased freshwater yield compared to TSS alone. The enhancement in yield ranged from 20.93% to 81.39% for TSS with SHSMs in comparison to TSS, establishing it as a promising option for sustainable freshwater production.
- TSS-S exhibits a notable improvement of approximately 75.12% in energy efficiency, whereas TSS-NB and TSS-B demonstrate enhancements of about 29.92% and 16.07%, respectively, compared to TSS.
- Exergy efficiency increases by approximately 36.44%, 8.41%, and 7.47% for TSS-S, TSS-NB, and TSS-B, respectively, in comparison to TSS.
- Economic assessment demonstrated a noteworthy decrease in CPL, reaching up to 42.86% (TSS-S), and a corresponding reduction in the payback period by as much as 44.33% (TSS-S) with the integration of SHSM. This leads to the conclusion that incorporating SHSMs into TSS is both a cost-effective and environmentally sustainable method for producing fresh water.
- The improvement potential and sustainability index for the examined cases lie within the ranges of 98.63–98.85 and 1.01–1.014, respectively.

- The TDS and pH levels of the fresh water generated from TSS adhere to the recommended ranges outlined by the WHO. Consequently, the obtained fresh water is suitable for domestic applications.

The current study could be expanded by integrating PCM with SHSMs to notably improve the performance of the solar desalination system. Additionally, the efficiency of TSS could be further enhanced by incorporating a pulsating heat pipe along with SHSMs. Exploring diverse glass cover cooling techniques in conjunction with SHSMs could be seen as a further scope of future research for improving the freshwater generation from TSS.

## Nomenclature

$A_t$	TSS basin area (m <sup>2</sup> )
$C_{AFC}$	Annual fixed cost
$C_{AOMC}$	Annual operational and maintenance cost
$C_{ASV}$	Annual salvage cost
$C_{CPL}$	Cost per liter
$C_{in}$	Initial cost
$C_{TAC}$	Total annual cost
$E_{x,in}$	Exergy input (kWh)
$E_{x,out}$	Exergy input (kWh)
$h_{fg}$	Latent heat of evaporation (J/kg)
$i$	Annual interest rate
$I_S$	Solar irradiation (W/m <sup>2</sup> )
$M_a$	Annual freshwater yield
$m_w$	Yield (L/m <sup>2</sup> )
$n$	Lifespan
$N_d$	Number of sunny days (330 days for New Delhi)
$P_p$	Payback period
$T_{amb}$	Ambient temperature (K)
$T_{sun}$	Sun temperature (6000 K)
$\eta_{en}$	Thermal efficiency
$\eta_{ex}$	Exergy efficiency

## Abbreviations

IP	Improvement potential
PCM	Phase change material

SI	Sustainability Index
SHSMs	Sensible heat storage materials
TSS	Triangular solar still
TSS-B	Triangular solar still with bricks
TSS-NB	Triangular solar still with paper napkins wrapped around the brick
TSS-S	Triangular solar still with sand bed

## Declaration of interests

The authors do not work for, advise, own shares in, or receive funds from any organization that could benefit from this article, and have declared no affiliations other than their research organizations.

## Funding

The research underpinning this publication was undertaken independently and was not contingent upon any external financial endorsements or grants.

## Acknowledgments

The authors would like to thank the Department of Mechanical Engineering, Netaji Subhas University of Technology, New Delhi, for giving them the opportunity to use their resources and work in such a challenging environment.

## References

- [1] WHO & UNICEF, *Progress on Drinking Water, Sanitation and Hygiene*, WHO and UNICEF, 2017, <https://washdata.org/sites/default/files/documents/reports/2018-01/JMP-2017-report-final-highlights.pdf>, 1-6 pages.
- [2] M. O. Aijaz, M. R. Karim, M. H. D. Othman, U. A. Samad, *Desalination*, 2023, **553**, article no. 116475.
- [3] M. Charbti, C. Fortin, M. Mezni, M. T. Hadjyoussef, M. B. Zayani, *C. R. Chim.*, 2022, **25**, 293-309.
- [4] K. Hosni, K. Mahmoudi, M. Haraketi, S. Jellali, E. Srasra, *C. R. Chim.*, 2023, **26**, 113-128.
- [5] L. Aref, R. Fallahzadeh, V. M. Avargani, *Energy Convers. Manag.*, 2021, **228**, article no. 113694.
- [6] S. Baloda, M. K. Soni, N. Sharma, *Int. J. Ambient. Energy*, 2023, **44**, 542-554.
- [7] R. Jain, *Clean Technol. Environ. Policy*, 2012, **14**, 1-4.
- [8] N. Sharma, R. Choudhary, *Solar Energy: Systems, Challenges, and Opportunities*, Springer, Singapore, 2020, 77-93 pages.
- [9] V. Sunil, N. Sharma, *J. Therm. Anal. Calorim.*, 2014, **118**, 523-531.

- [10] T. V. Arjunan, H. Ş. Aybar, N. Nedunchezian, *Renew. Sustain. Energy Rev.*, 2009, **13**, 2408-2418.
- [11] O. Bait, M. Si-Ameur, *Energy*, 2016, **98**, 308-323.
- [12] O. Younis, A. K. Hussein, M. E. H. Attia *et al.*, *Energy Rep.*, 2022, **8**, 8236-8258.
- [13] O. Bait, *Solar Energy*, 2024, **269**, article no. 112322.
- [14] O. Younis, A. K. Hussein, M. E. H. Attia *et al.*, *Sustainability (Switzerland)*, 2022, **14**, article no. 10136.
- [15] K. Ramzy, M. Abdelgaleel, A. E. Kabeel, H. Mosalam, *Environ. Sci. Pollut. Res.*, 2023, **30**, 72398-72414.
- [16] H. S. Deshmukh, S. B. Thombre, *Desalination*, 2017, **410**, 91-98.
- [17] M. Abdelgaleel, E. Ahmed abdelAziz, H. Mosalam, A. E. Kabeel, M. Alswat, K. Ramzy, *Solar Energy*, 272, **2024**, article no. 112469.
- [18] P. N. Kumar, A. M. Manokar, B. Madhu, A. E. Kabeel, T. Arunkumar, H. Panchal, R. Sathyamurthy, *Groundwat. Sustain. Dev.*, 2017, **5**, 229-234.
- [19] K. V. Modi, D. B. Ankoliya, D. L. Shukla, *J. Renew. Sustain. Energy*, 2018, **10**, article no. 043708.
- [20] A. E. Kabeel, Y. Taamneh, R. Sathyamurthy, P. Naveen Kumar, A. M. Manokar, T. Arunkumar, *Heat Transf. Asian Res.*, 2019, **48**, 100-114.
- [21] A. M. Manokar, Y. Taamneh, A. E. Kabeel *et al.*, *Groundwat. Sustain. Dev.*, 2020, **10**, article no. 100319.
- [22] A. A. Azooz, G. G. Younis, *J. Renew. Sustain. Energy*, 2016, **8**, article no. 033702.
- [23] A. E. Kabeel, M. Abdelgaied, N. Almulla, *2016 7th International Renewable Energy Congress (IREC)*, IEEE, New York, 2016, 1-6 pages.
- [24] M. Feilzadeh, M. Soltanieh, M. R. K. Estahbanati, K. Jafarpur, S. Ashrafmansouri, *Desalination*, 2017, **424**, 1-10.
- [25] B. Jamil, N. Akhtar, *Environ. Prog Sustain. Energy*, 2019, **38**, article no. 13227.
- [26] O. Bait, M. Si-Ameur, *Energy*, 2017, **141**, 818-838.
- [27] M. Appadurai, V. Velmurugan, *Sustain. Energy Technol. Assess.*, 2015, **9**, 30-36.
- [28] M. El-Naggar, A. A. El-Sebaei, M. R. I. Ramadan, S. Aboul-Enein, *Desalination Water Treat.*, 2016, **57**, 17151-17166.
- [29] N. Sharma, S. Noushad, G. Siva Ram Kumar Reddy, in *Recent Trends in Thermal Engineering* (R. Kumar, A. K. Pandey, R. K. Sharma, G. Norkey, eds.), Lecture Notes in Mechanical Engineering, Springer, Singapore, 2022, 83-91.
- [30] S. S. Tuly, M. S. Islam, R. Hassan, B. K. Das, M. R. I. Sarker, *Case Stud. Therm. Eng.*, 2022, **37**, article no. 102256.
- [31] H. Panchal, A. Sohani, N. V. Nguyen *et al.*, *Environ. Sci. Pollut. Res.*, 2023, **30**, 11769-11784.
- [32] A. E. Kabeel, M. Abdelgaied, *DES*, 2016, **383**, 22-28.
- [33] S. M. Shalaby, E. El-bialy, A. A. El-sebaei, *Desalination*, 2016, **398**, 247-255.
- [34] E. A. Abdel-Aziz, T. M. Mansour, M. M. K. Dawood, T. M. Ismail, K. Ramzy, *Environ. Sci. Pollut. Res.*, 2023, **30**, 66135-66156.
- [35] S. Shoeibi, M. Saemian, S. M. Parsa, M. Khiadani, S. A. A. Mirjalily, H. Kargarsharifabad, *Desalination*, 2023, **567**, article no. 116955.
- [36] A. Hemmatian, H. Kargarsharifabad, A. A. Esfahlani, N. Rahbar, S. Shoeibi, *Solar Energy*, 269, **2024**, article no. 112371.
- [37] S. Shoeibi, M. Saemian, M. Khiadani, H. Kargarsharifabad, S. A. A. Mirjalily, *Energy Convers. Manage.*, 276, **2023**, article no. 116504.
- [38] B. Omid, N. Rahbar, H. Kargarsharifabad, Z. P. Moziraji, *Energy Conver. Manage.*, 2023, **292**, article no. 117347.
- [39] S. Shanmugan, S. Palani, B. Janarthanan, *Desalination*, 2018, **433**, 186-198.
- [40] M. E. H. A. Attia, M. Shajahan, M. M. Athikesavan, A. Kadhim Hussein, E. Elaloui, H. Togun, L. Kolsi, *Iran. J. Chem. Chem. Eng.*, 2024, **43**, 1792-1809.
- [41] S. Shoeibi, S. Ali Agha Mirjalily, H. Kargarsharifabad, H. Panchal, R. Dhivagar, *Environ. Sci. Pollut. Res.*, 2022, **29**, 65353-65369.
- [42] A. E. Kabeel, S. A. El-agouz, R. Sathyamurthy, T. Arunkumar, *Desalination*, 2018, **443**, 122-129.
- [43] P. Pal, R. Dev, D. Singh, A. Ahsan, *Desalination*, 2018, **447**, 55-73.
- [44] M. S. Yousef, H. Hassan, H. Sekiguchi, *Appl. Therm. Eng.*, 2019, **150**, 30-41.
- [45] A. M. Manokar, M. Vimala, D. Prince Winston, D. R. Rajendran, R. Sathyamurthy, A. E. Kabeel, *Heat Transf.*, 2020, **49**, 4394-4409.
- [46] M. Elashmawy, *Desalination*, 2020, **473**, article no. 114182.
- [47] A. E. Kabeel, K. Harby, M. Abdelgaied, A. Eisa, *Solar Energy*, 2021, **217**, 187-199.
- [48] S. Shoeibi, M. Saemian, H. Kargarsharifabad, S. Hosseinzade, N. Rahbar, M. Khiadani, M. M. Rashidi, *Int. Commun. Heat Mass Transf.*, 2022, **138**, article no. 106387.
- [49] M. El, H. Attia, A. Elnaby, *Heat Transf.*, 2020, **50**, 768-783.
- [50] R. Dhivagar, *Energy Sci. Eng.*, 2022, **10**, 3154-3166.
- [51] D. Mevada, H. Panchal, M. Ahmadein, M. E. Zayed, *Case Stud. Therm. Eng.*, 2022, **29**, article no. 101687.
- [52] O. Bait, *J. Clean. Prod.*, 2019, **212**, 630-646.
- [53] S. Shoeibi, N. Rahbar, A. Abedini Esfahlani, H. Kargarsharifabad, *J. Ther. Anal. Calorimet.*, 2022, **147**, 9645-9660.
- [54] R. Dhivagar, S. Shoeibi, S. M. Parsa, S. Hoseinzadeh, H. Kargarsharifabad, M. Khiadani, *Renew. Energy*, 2023, **206**, 879-889.
- [55] T. Mahala, N. Sharma, *Desalination*, 2024, **578**, article no. 117467.
- [56] K. S. Shibib, H. I. Qatta, M. S. Hamza, *Therm. Sci.*, 2013, **17**, 1119-1123.
- [57] S. Kumar, A. K. Sahu, M. Kumar, *Water Sci. Technol.*, 2021, **84**, 2760-2779.
- [58] J. F. Łatka, A. Jasiołek, A. Karolak *et al.*, *J. Build. Eng.*, 2022, **50**, article no. 104135.
- [59] N. Sharma, N. Shaik, V. Kumar, M. Kumar, in *Thermal Energy Systems* (A. Kumar, V. P. Singh, C. S. Meena, N. Dutt, eds.), Taylor & Francis, Boca Raton, 1st ed., 2023, 141-153.
- [60] S. Shoeibi, N. Rahbar, A. A. Esfahlani, H. Kargarsharifabad, *Renewable Energy*, 2021, **171**, 227-244.
- [61] R. Hassan, H. Barua, B. K. Das, *Energy Sci. Eng.*, 2021, **9**, 2232-2251.
- [62] S. Hossain, H. Chowdhury, T. Chowdhury, J. Uddin, *Energy Rep.*, 2020, **6**, 868-878.